Journal of Theoretical Biology 253 (2008) 333–344

Contents lists available at ScienceDirect

Journal of Theoretical Biology

journal homepage: www.elsevier.com/locate/yjtbi

Brain cooling maintenance with cooling cap following induction with intracarotid cold saline infusion: A quantitative model

Matthew A. Neimark [a,b,*], Angelos-Aristeidis Konstas [c,b], Jae H. Choi [b], Andrew F. Laine [a,b], John Pile-Spellman [b]

[a] Department of Biomedical Engineering, Columbia University, 1210 Amsterdam Avenue, New York, NY 10027, USA
[b] Department of Radiology, Columbia University, 177 Fort Washington Avenue, New York, NY 10032, USA
[c] Department of Radiology, Massachusetts General Hospital, Fruit Street, Boston, MA 02114, USA

ARTICLE INFO

Article history:
Received 13 November 2007
Received in revised form
18 February 2008
Accepted 25 March 2008
Available online 27 March 2008

Keywords:
Intracarotid saline infusion
Selective brain cooling
Cooling cap
Hemodilution
Intravascular volume loading

ABSTRACT

Intracarotid cold saline infusion (ICSI) is potentially much faster than whole-body cooling and more effective than cooling caps in inducing therapeutic brain cooling. One drawback of ICSI is hemodilution and volume loading. We hypothesized that cooling caps could enhance brain cooling with ICSI and minimize hemodilution and volume loading. Six-hour-long simulations were performed in a 3D mathematical brain model. The Pennes bioheat equation was used to propagate brain temperature. Convective heat transfer through jugular venous return and the circle of Willis was simulated. Hemodilution and volume loading were modeled using a two-compartment saline infusion model. A feedback method of local brain temperature control was developed where ICSI flow rate was varied based on the rate of temperature change and the deviation of temperature to a target (32 °C) within a voxel in the treated region of brain. The simulations confirmed the inability of cooling caps alone to induce hypothermia. In the ICSI and the combination models (ICSI and cap), the control algorithm guided ICSI to quickly achieve and maintain the target temperature. The combination model had lower ICSI flow rates than the ICSI model resulting in a 55% reduction of infusion volume over a 6 h period and higher hematocrit values compared to the ICSI model. Moreover, in the combination model, the ICSI flow rate decreased to zero after 4 h, and hypothermia was subsequently maintained solely by the cooling cap. This is the first study supporting a role of cooling caps in therapeutic hypothermia in adults.
© 2008 Elsevier Ltd. All rights reserved.

1. Introduction

Hypothermia has been shown to reduce infarct volume and improve neurologic outcomes in animal models of focal cerebral ischemia (Chen et al., 1992). It has also improved survival and functional outcomes in randomized clinical trials involving patients with global cerebral ischemia after cardiac arrest (Bernard et al., 2002; The Hypothermia After Cardiac Arrest (HACA) Study Group, 2002). In most clinical studies, hypothermia is induced by surface cooling. While this is the simplest and most cost-effective method of inducing hypothermia (Feigin et al., 2003), it has a major limitation. Surface cooling requires 3–7 h to reach the target brain temperature of 32–34 °C (Kammersgaard et al., 2000; Schwab et al., 2001). Although intravenous whole-body cooling may be able to accelerate the induction of hypothermia, this method is still reported require 2–4.5 h to achieve target temperature (Georgiadis et al., 2001) Further, in clinical trials of this method not all patients were cooled to target temperature (De Georgia et al., 2004; Lyden et al., 2005). Hundreds of animal studies on hypothermia induction, as well as randomized trials on intravenous thrombolysis have demonstrated the efficacy of treatment only within 3 h after the onset of symptoms (The National Institute of Neurological Disorders and Stroke rt-PA Stroke Study Group, 1995; Konstas et al., 2006). Hence, whole-body cooling induction will miss the 3-h therapeutic window in the majority of stroke patients.

Selective brain cooling (SBC) may be able to induce hypothermia faster than whole-body cooling methods. Different methods for SBC exist (Harris and Andrews, 2005). The non-invasive methods most commonly used are cooling caps and helmets. However, theoretical analyses (Diao et al., 2003; Nelson and

Abbreviations: A1, proximal segment of anterior cerebral artery; A2, distal segment of anterior cerebral artery; ACA, anterior cerebral artery; BA, basilar artery; CoW, circle of willis; ICA, internal carotid artery; *HCT*, hematocrit; *IAT*, ipsilateral anterior territory; ICSI, intracarotid cold saline infusion; *MAP*, mean arterial pressure; MCA, middle cerebral artery; P1, proximal segment of posterior cerebral artery; P2, distal segment of posterior cerebral artery; PCA, posterior cerebral artery; SBC, selective brain cooling.

* Corresponding author at: Department of Biomedical Engineering, Columbia University, 1210 Amsterdam Avenue, New York, NY 10027, USA.
Tel.: +1 212 854 5996; fax: +1 212 854 5995.
E-mail address: man2003@columbia.edu (M.A. Neimark).

0022-5193/$ - see front matter © 2008 Elsevier Ltd. All rights reserved.
doi:10.1016/j.jtbi.2008.03.025

Nomenclature

∇	gradient operator
$\nabla\cdot$	divergence operator
∂	partial differentiation operator
$\iiint$	volume integration
ρ	density ($kg\,m^{-3}$)
κ	control constant ($m^3\,s^{-1}\,{}^{\circ}C^{-1}$)
π	≈ 3.1416
τ	time constant (s)
η	viscosity ($kg\,m^{-1}\,s^{-1}$)
Δ	change from baseline
ω	cerebral blood perfusion ($ml\,min^{-1}\,hg^{-1}$)
c	heat capacity ($J\,kg^{-1}\,K^{-1}$)
d	differentiation operator, vessel diameter (m)
e	≈ 2.7183
h	convective heat transfer coefficient
H	catheter heat transfer coefficient ($m^3\,s^{-1}$), heat (J)
k	heat conductivity ($W\,m^{-1}\,K^{-1}$)
k	flow rates, and flow rate parameters for hemodilution model ($m^3\,s^{-1}$)
m	mass (kg)
q	metabolism, heat production ($W\,m^{-3}$)
r	radius
$\vec{r}$	three-dimensional spatial location
t	time (s)
F	flow ($m^3\,s^{-1}$)
G	vascular conductivity ($kg^{-1}\,m^4\,s$)
L	vessel length (m)
P	pressure ($kg\,m^{-1}\,s^{-2}$)
T	temperature (°C)
V	volume (m^3)

Subscripts

0	baseline
1	arbitrary adjacent vessel junctions (P), intravascular fluid space (v, V)
2	arbitrary adjacent vessel junctions (P), peripheral fluid space (v, V)
b	basal fluid loss
cACA	contralateral anterior cerebral artery
cMCA	contralateral middle cerebral artery
cPCA	contralateral posterior cerebral artery
i	infusion flow (k)
ICA	internal carotid artery
iACA	ipsilateral anterior cerebral artery
iMCA	ipsilateral middle cerebral artery
iPCA	ipsilateral posterior cerebral artery
B	combined basilar and verterbral (G)
IV	Intravascular
*IV*0	baseline intravascular
r	urine flow rate parameter
RBC	red blood cell
t	transfer flow parameter between intravascular and peripheral volumes

Nunneley, 1998; Sukstanskii and Yablonskiy, 2007) and empirical measurements (Corbett and Laptook, 1998; Mellergard, 1992; Wang et al., 2004; Zhu et al., 2006) suggest that they are only effective in reducing the temperature in superficial cerebral regions and not deep brain structures. These studies demonstrated that head surface cooling is ill conceived because brain is highly perfused by warm blood, which severely limits the conductive penetration of surface cooling. Another SBC method is intracarotid cold saline infusion (ICSI) where cold saline is infused into the internal carotid artery (ICA) via transfemoral catheterization. This method is potentially much faster than whole-body cooling and more effective than surface SBC. Two recent theoretical studies addressed the clinical feasibility of ICSI for inducing hypothermia (Konstas et al., 2007; Neimark et al., 2007). A three-dimensional mathematical model was developed to examine the transient and steady-state temperature distribution in the human brain during ICSI. A healthy brain and a brain with ischemic stroke were modeled. The complete Circle of Willis (CoW) and two common CoW variants were incorporated in the model, taking into account the effect of cooled jugular venous blood returning to the body core. In the simulations, an infusion rate of $30\,ml\,min^{-1}$ was sufficient to induce moderate hypothermia (defined as 32–34 °C) within 5–10 min in the ipsilateral hemisphere. These theoretical analyses suggested that this efficiency of hypothermia induction was also efficient in brains with stroke and/or common CoW variants.

The drawback of ICSI is the length of time hypothermia can be maintained due to safety concerns. One such concern is the increasing local and systemic hemodilution that results from a constant infusion of $1800\,ml\,h^{-1}$ of isotonic saline. One effect of brain cooling is an exponential decrease of cerebral perfusion due to coupling of metabolism, and perfusion in the brain (Ehrlich et al., 2002). It is conceivable that if head surface cooling were to be attempted in addition to ICSI, cerebral perfusion in the brain would be further decreased enough in the head so that less saline would need to be infused to induce and maintain SBC.

In the present study, a method of controlling brain temperature by modulating cold saline flow during SBC is presented. If SBC is to be implemented clinically, it will be necessary to utilize control methods that maintain brain temperature at a target temperature over the length of the therapy period. This control method also allows comparison between cooling protocols involving ICSI alone, and combination ICSI and cooling cap by comparing the amount of saline flow necessary to maintain target temperature.

Three different methods of SBC are simulated theoretically: Cooling cap alone, ICSI alone and a combination of ICSI and cooling cap. In methods involving ICSI, the control algorithm was employed to target and maintain hypothermia at 32 °C. This temperature was utilized because it was the lowest target temperature employed in human hypothermia stroke trials (Krieger et al., 2001) and as such would provide the largest challenge in terms of maintaining safe intravascular volumes and hematocrits. In the simulation, hypothermia was continued for 6 h, the minimum time-length of hypothermia maintenance in pilot human studies (Kammersgaard et al., 2000). This study addresses three questions concerning SBC: First, whether the control algorithm can guide saline infusion to quickly achieve target temperature and maintain it in a stable fashion. Second, whether utilization of a cooling cap can enhance brain cooling with ICSI. Third, if the cooling cap application can minimize the ICSI flow rate with subsequent reduction in the degree of hemodilution resulting from ICSI during the 6-h hypothermia maintenance.

2. Methods

2.1. Brain model

A 3D hemispheric head model was developed in spherical coordinates. This model consists of four tissue layers: white

matter, gray matter, skin, and bone (Fig. 1A, B). For every coordinate within the head model, there was an associated variable temperature T, metabolism q, and perfusion ω. Constant biothermal parameters corresponding to each coordinate were density ρ, specific heat c, and thermal conductivity k. These physical and physiological properties, as published in previous studies, were used for each of the tissue layers, blood and saline (Table 1).

In the brain tissues, metabolism and perfusion are related to temperature and hematocrit by

$$q = q_0 \cdot 3.0^{0.084(T-37)} \quad (1)$$

and

$$\omega = \omega_0 \cdot 3.0^{0.084(T-37)}(1 - 2.2\Delta_{HCT}) \quad \text{(Konstas et al., 2007)} \quad (2)$$

due to metabolic coupling. In the skull and scalp these two parameters are constant. Below 28 °C, flow is no longer coupled to temperature (Michenfelder and Milde, 1991), so the equation becomes

$$\omega = \omega_0 \cdot 3.0^{0.084(-9)}(1 - 2.2\Delta_{HCT}) \quad (3)$$

Temperature in the model evolved according to the Pennes bioheat equation:

$$\frac{\partial T(\vec{x},t)}{\partial t} = \frac{\nabla \cdot [k(\vec{x})\nabla T(\vec{x},t)]}{\rho(\vec{x})c(\vec{x})} + \frac{\rho_{blood}c_{blood}}{\rho(\vec{x})c(\vec{x})}\omega(\vec{x},t) \times [T_{artery}(\vec{x},t) - T(\vec{x},t)] + \frac{q(\vec{x},t)}{\rho(\vec{x})c(\vec{x})} \quad \text{(Pennes, 1948)} \quad (4)$$

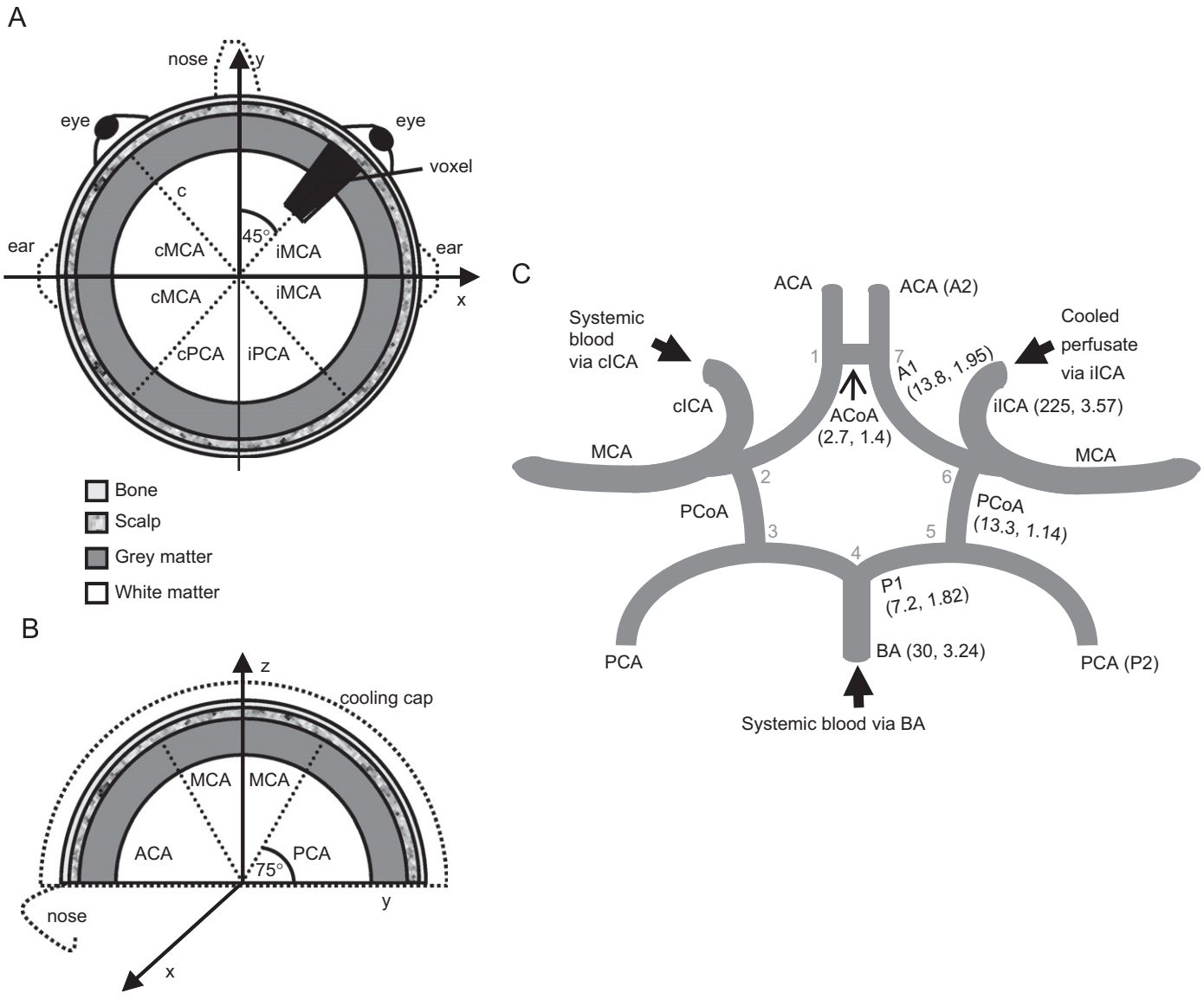

Fig. 1. Anatomic layout of the head model. (A) Axial section at the base of the brain with the demarcation of the vascular territories (ACA—anterior cerebral artery; MCA—middle cerebral artery; PCA—posterior cerebral artery). The letters "i" and "c" prior to the vessel abbreviation signify, respectively, either the side ipsilateral or contralateral to the infused vessel. (B) Para-median section of the model. The dotted line represents the cooling cap that was used in some of the simulations. (C) Simplified 2D circle of Willis geometry (A1—proximal portion of ACA; A2—distal portion of ACA; P1—proximal portion of PCA; P2—distal portion of PCA). The numbers 1–7 (in gray) correspond to the subscripted numbers in Eq. (10). The numbers in parentheses next to each vessel are, respectively, the length and diameter in millimeters of each vessel (Neimark et al., 2007).

where $\vec{x}$ is the spatial coordinate and T_{artery} is the temperature of the blood that perfuses the tissue at that point.

At the surface of the head model, heat transfer was described by the following boundary condition:

$$k\frac{\partial T}{\partial r} = -h(T - T_{medium}) \tag{5}$$

where h is the heat transfer coefficient between the scalp and the medium surrounding it (T_{medium}). For air $T_{medium} = 25\,^{\circ}C$ and $h = 8\,W\,m^{-2}\,K^{-1}$) (Diao et al., 2003). To determine realistic values for T_{medium} and h for the cooling cap, data from a previous cooling cap study in which scalp temperature was measured (Corbett and Laptook, 1998) was employed. In this study, T_{medium} was directly measured as 4 °C. To determine h, different values of h were varied in the mathematical cranial model, until the simulation yielded a surface scalp temperature of 15.8 °C after 50 min, as reported in this experimental study. The ultimate value of h used to represent the cooling cap was $= 77\,W\,m^{-2}\,K^{-1}$).

Further details of the brain model, including boundary conditions for solving Eq. (4) have been previously described (Konstas et al., 2007).

2.2. Saline infusion

Saline was infused through the ipsilateral ICA. There, it mixed with the inflowing blood, forming a perfusate with temperature:

$$T_{ICA} = \frac{\rho_{blood}c_{blood}F_{ICA}\cdot T_{core} + \rho_{saline}c_{saline}F_{saline}\cdot T_{saline}}{\rho_{blood}c_{blood}F_{ICA} + \rho_{saline}c_{saline}F_{saline}} \tag{6}$$

and hematocrit

$$HCT_{ICA} = \frac{F_{ICA}\cdot HCT_{systemic}}{F_{ICA} + F_{saline}} \tag{7}$$

where F_{ICA} is blood flow rate in the ipsilateral ICA and F_{saline} is the saline flow rate.

2.3. Circle of Willis model

Mixed cold saline and blood perfusate further mixed with blood from the contralateral ICA and basilar artery (Fig. 1C). The CoW was modeled according to a linear circuit equation. Flow in the in any vessel segment of the model was determined by the pressure of the two endpoints, P_1 and P_2, according Pousseuille's law:

$$F = G(P_2 - P_1) \tag{8}$$

where vascular conductivity, G, was determined by

$$G = \frac{\pi d^4}{128\eta_{blood}L} \tag{9}$$

where d is vessel diameter, L is vessel length, and η_{blood} is blood viscosity.

Kirchoff's pressure and flow laws were used to determine pressure node values P_1–P_7 (Fig. 1C) in the CoW which were interrelated to incoming flows into each of the cerebral vascular territories, according to the following matrix equation:

$$\begin{bmatrix} -G_{12}-G_{17} & G_{12} & 0 & 0 & 0 & 0 & G_{17} \\ G_{12} & -G_{12}-G_{23}-G_{ICA} & G_{23} & 0 & 0 & 0 & 0 \\ 0 & G_{23} & -G_{23}-G_{34} & G_{34} & 0 & 0 & 0 \\ 0 & 0 & G_{34} & -G_{34}-G_{45}-G_{BA} & G_{45} & 0 & 0 \\ 0 & 0 & 0 & G_{45} & -G_{45}-G_{56} & G_{56} & 0 \\ 0 & 0 & 0 & 0 & G_{56} & -G_{56}-G_{67}-G_{ICA} & G_{67} \\ G_{17} & 0 & 0 & 0 & 0 & G_{67} & -G_{17}-G_{67} \end{bmatrix} \begin{bmatrix} P_1 \\ P_2 \\ P_3 \\ P_4 \\ P_5 \\ P_6 \\ P_7 \end{bmatrix} = \begin{bmatrix} F_{cACA} \\ F_{cMCA} - MAP\cdot G_{ICA} \\ F_{cPCA} \\ -MAP\cdot G_B \\ F_{iPCA} \\ F_{iMCA} - MAP\cdot G_{ICA} \\ F_{iACA} \end{bmatrix} \tag{10}$$

In this equation, F_{iACA}, F_{cACA}, F_{iMCA}, F_{cMCA}, F_{iPCA}, F_{cPCA} are flows of vessels supplying separate vascular territories and were calculated by

$$F = \iiint_{Territory} \omega\, dV \tag{11}$$

Conductance values of vessels in the CoW have double digit subscript values representing the two nodes which are their endpoints (Fig. 1C). Conductance values of the ICA and combined basilar and vertebral arteries are represented by G_{ICA} and G_B. Eq. (8) was used to calculate all conductance values. *MAP* is mean arterial pressure (95 mm Hg).

Eq. (10) was inverted to determine P_1–P_7 and the flows in each of the CoW vessels, ICA, and basilar artery (BA) arteries were calculated with Eq. (8). These flows were used to determine mixing of blood and cold saline which determine temperature and hematocrit of the blood which supplied the vascular territories from the anterior cerebral artery (ACA), middle cerebral artery (MCA), and posterior cerebral artery (PCA) vessels (Neimark et al., 2007). Methods describing how this hematocrit and temperature were calculated, along with anatomical details regarding size of the vessels in the CoW which determine vascular conductance, and how blood viscosity is calculated have been presented in greater detail in a previous study (Neimark et al., 2007).

Table 1
Physical and physiological properties of the model

Anatomic structure of the head	Specific heat c ($J\,kg^{-1}\,K^{-1}$)	Mass density ρ ($kg\,m^{-3}$)	Thermal conductivity k ($W\,m^{-1}\,K^{-1}$)	Perfusion ω_0 [$ml\,(min\,100\,g)^{-1}$]	Metabolic rate q_o ($W\,m^{-3}$)	Radius r (mm)
Saline	4213	1006	0.5	N/A	N/A	N/A
Blood	3800	1050	0.5	N/A	N/A	N/A
Scalp	4000	1000	0.342	2.0	363.4	93
Bone	2300	1520	1.16	1.8	368.3	89
Gray matter	3700	1030	0.49	80	16 700	85
White matter	3700	1030	0.49	20	4175	67

Values obtained from Diao et al. (2003), Nelson and Nunneley (1998), Van Leeuwen et al. (2000), Xu et al. (1999). N/A: Non-applicable.

2.4. Systemic Hemodilution model

Hemodilution was modeled using a two compartment saline infusion model (Drobin and Hahn, 2002). In this model, volume changes to intravascular and peripheral volumes respond to an intravascular infusion with flow rate of k_i as follows:

$$\frac{dv_i}{dt} = k_i - k_b - k_r\frac{v_i - V_i}{V_i} - k_t\left(\frac{v_i - V_i}{V_i} - \frac{v_p - V_p}{V_p}\right) \tag{12}$$

$$\frac{dv_p}{dt} = k_t\left(\frac{v_i - V_i}{V_i} - \frac{v_p - V_p}{V_p}\right) \tag{13}$$

where v_i and v_p are, respectively, time-varying intravascular and peripheral volumes, $V_i = 4.0\,L$ and $V_p = 6.9\,L$ (Drobin and Hahn, 2002) are, respectively, baseline intravascular (plasma) and peripheral volumes, $k_t = 160\,ml\,min^{-1}$ is the flow rate parameter regulating transfer between the intravascular and peripheral spaces, $k_r = 27\,ml\,min^{-1}$ is the urine flow rate parameter, and $k_b = 0.5\,ml\,min^{-1}$ is the basal loss parameter. Urine flow was determined by the term in Eq. (12) $k_r(v_i - V_i)/V_i$.

Subsequent to infusion, hematocrit can be determined by

$$HCT_{systemic} = \frac{V_{RBC}}{v_i + V_{RBC}} \tag{14}$$

and $v_i + V_{RBC}$ is the total intravascular volume.

Initial hematocrit was set to 42%, so red blood cell volume is $V_{RBC} = HCT_{systemic}V_i/(1 - HCT_{systemic})$ which is 2.9 L.

2.5. Venous return

Cooled venous blood returns from the head and cools the body according to

$$\frac{dT_{core}}{dt} = \frac{\rho_{blood}c_{blood}(T_{venous} - T_{core})\int\int\int_{brain\ model}\omega(\vec{r})\,d\,\vec{r}}{m_{body}c_{body}} \tag{15}$$

where T_{venous} is the average venous return temperature, $m_{body} = 70\,kg$ is body mass and $c_{body} = 3475\,J\,kg^{-1}\,K^{-1}$. Since blood and brain tissues achieve thermal equilibrium (Baish, 2000), venous return temperatures were calculated by integrating the product of the brain temperature and blood perfusion over the entire brain model as follows (Fiala et al., 1999):

$$T_{venous} = \iiint_{Brain\ Model}\omega(\vec{r})T(\vec{r})\,d\,\vec{r} \Big/ \iiint_{Brain\ Model}\omega(\vec{r})\,d\,\vec{r} \tag{16}$$

Core temperature was used in Eqs. (6), (19), (22), and (23), and was also the blood temperature in the contralateral ICA and BA which were in turn utilized to determine mixing temperatures in the CoW.

2.6. Control of saline infusion

The control procedure involved attempting to force the temperature to follow an exponential profile. These were chosen for several reasons: First, exponential functions are parametically simple and for this particular application, can be specified in terms of its time constant (which determines how quickly the temperature reaches the target). Second, exponentials are naturally easy to control in that the rate of temperature change can be gradually diminished as the temperature approaches the target. Also, ICSI temperature responses with a constant flow infusion had an approximately exponential profile, although a true steady state was never reached (Konstas et al., 2007; Neimark et al., 2007), and therefore control manipulations could be minimized. The goal of this temperature control procedure was to (1) control the flow during the initial stages of infusion to achieve target temperature within a desired time period, and (2) maintain the achieved target temperature.

Temperature was monitored in a 9.6 ml elongated voxel located in the middle of the ipsilateral anterior territory (45° from the base of the brain in the azimuth direction and 45° in the anterior direction from the anterior-posterior midline; see Fig. 1A) and containing approximately half white matter and half gray matter, and extending through the entire radius of gray matter. In principle, MR spectroscopy could be used to non-invasively measure the temperature in this voxel (Childs et al., 2007). In the model, T_{voxel}, was the average temperature in the volume of this voxel, and was sampled in the simulation once per second.

The desired temperature profile of the voxel is an exponential expressed as

$$T_{voxel}(t) = (T_{voxel0} - T_{target})e^{-t/\tau_{desired}} + T_{target} \tag{17}$$

where T_{voxel0} is the initial voxel temperature, T_{target} is the target temperature, and $\tau_{desired}$ is the desired time constant of cooling (i.e. the time by which 63% of cooling should have taken place).

Eq. (17) is the solution to the differential equation:

$$\frac{dT_{voxel}}{dt} - \frac{(T_{target} - T_{voxel})}{\tau_{desired}} = 0 \tag{18}$$

Therefore, any difference between dT_{voxel}/dt and $(T_{target} - T_{voxel})/\tau_{desired}$ implied that that the voxel cooling was not cooling according to the desired speed. Further, after T_{target} has been achieved, dT_{voxel}/dt should be zero.

There are two parameters in ICSI which can be altered to affect brain temperature: (1) infusate inflow temperature and (2) infusate flow rate. Outflow saline temperature relates to these parameters according to

$$T_{saline} = (T_{saline\_in} - T_{core})e^{-H_{cath}/F_{saline}} + T_{core} \tag{19}$$

where T_{saline_in} is the saline temperature infused at the beginning of the catheter, T_{saline} is the outflow saline, as in Eq. (6), and H_{cath}

is the normalized heat transfer coefficient between the catheter and body. For a derivation of Eq. (19), see Appendix A. H_{cath} is dependent on many several factors including length, radius, and insulating properties of the catheter. For this study H_{cath} was determined empirically from data measured from a previous study (Konstas et al., 2007) where a 5F insulated catheter was introduced into the femoral artery of a life-size human arterial tree polymer model (Flowtek, Boulder Colorado) and maneuvered until its tip was just inside the ICA past the carotid bifurcation. This vascular model was filled with circulating body temperature water and placed in a warm water bath, and freezing cold saline was pumped through the catheter. Temperature was measured at the catheter inflow, outflow, and in the arterial model. H_{cath} was determined for each flow rate tested with the following equation, which is Eq. (19) rearranged:

$$H_{cath} = -F_{saline} \ln\left(\frac{T_{saline} - T_{core}}{T_{saline\_in} - T_{core}}\right) \tag{20}$$

These individually determined H_{cath} values were then averaged to determine the general H_{cath} value utilized in Eq. (19). Data from the catheter flow experiment is shown in Table 2 which includes measurements at every tested flow rate of inlet temperature, arterial tree temperature, and outlet temperature. The table also includes calculated values of H_{cath}. H_{cath} was averaged to a value of 4.41 ml min^{-1}, which was subsequently used for all simulations. This value of H_{cath} was then used with Eq. (19) to calculate the expected saline outflow temperature (T_{saline_calc}) which could then be compared with the measured value of T_{saline} from the experiment (Table 2). The mean squared error between T_{saline} and T_{saline_calc} was 0.6 °C.

It is far more practical to modify infusate flow, rather than infusate temperature, during an ICSI procedure. However, the resultant temperature T_{voxel}, would be difficult to predict *a priori*. However, it is clear from previous studies (Konstas et al., 2007; Slotboom et al., 2004) and theoretical considerations, i.e. Eqs. (4), (6), and (19), that increasing F_{saline} should decrease dT_{voxel}/dt and vise versa. Further, although the exact relationship between ΔF_{saline} and dT_{voxel}/dt is unknown, it must be monotonic. Therefore, *modified according to*

$$\frac{dF_{saline}}{dt} = \kappa\left[\tau_{desired}\frac{dT_{voxel}}{dt} - (T_{target} - T_{voxel})\right] \tag{21}$$

where κ *is a constant which determines how quickly flow rate is modified to perturbations from the expected exponential profile. In our simulations,* $\tau_{desired} = 120\,s$ *and* $\kappa = 200\,ml\,min^{-1}\,°C^{-1}$. *Target temperature was 32 °C, saline inflow temperature was 0 °C, and initial flow rate was 50 ml min*$^{-1}$.

A flow diagram of the control model is shown in Fig. 2.

2.7. Simulations

There were three simulations performed in this study: (1) a simulation with cooling cap only and no saline infusion, (2) a simulation with saline infusion controlled to maintain average brain voxel temperature at 32 °C, and (3) a simulation with both cooling cap saline infusion controlled to maintain average brain voxel temperature at 32 °C. The simulations were stopped if target temperature was not reached within an hour since this would indicate that the particular method failed to achieve therapeutic hypothermia quickly enough.

Table 2
Experimental inlet and outlet temperatures and estimation of normalized heat transfer coefficient

Saline flow rate (F_{saline}), ml min^{-1}	Inlet temperature (T_{saline_in}), °C	Arterial tree temperature (T_{core}), °C	Measured outlet temperature (T_{saline}), °C	Calculated normalized heat transfer coefficient (H_{cath}), ml min^{-1}	Predicted outlet temperature (T_{saline_calc}), °C
50	−1.2	37.4	1.8	4.05	1.8
40	−1.3	37.0	2.5	4.18	2.4
30	−1.6	37.4	2.8	3.59	3.3
20	−1.7	36.4	5.0	3.87	5.3
10	−1.9	36.6	12.1	4.52	10.9

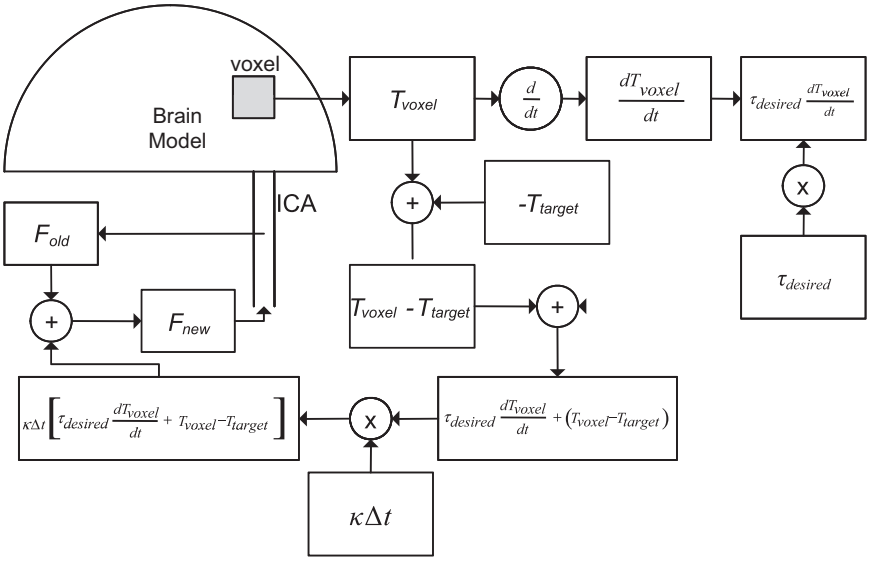

Fig. 2. Infusion flow control model. Voxel temperature is sampled. Its derivative, multiplied by the desired time constant, is compared with its deviation from the target temperature. This difference is then multiplied by $\kappa\Delta t$ and then added to the old saline flow rate F_{old} to determine the new flow rate F_{new}.

Simulations were performed in MATLAB with similar time steps and grid spacings of previous studies (Konstas et al., 2007; Neimark et al., 2007).

2.8. Calculation of cooling contributions

For the simulation with both cooling cap and saline infusion relative cooling contributions of the cooling cap and saline were calculated as follows: Between time points t_1 and t_2, the cooling effect of saline, in units of heat lost to the core, are as follows:

$$H_{Loss\_saline} = \int_{t_1}^{t_2} [T_{saline} - T_{core}(t)]F_{saline}(t)\,dt = -\int_{t_1}^{t_2} T_{core}(t)F_{saline}(t)\,dt \quad (22)$$

Total body heat loss can be calculated more directly as follows:

$$H_{Loss\_core} = c_{body}\int_{T_1}^{T_2} m_{body}(T_{core})\,dT_{core} \quad (23)$$

where $T_1 = T_{core}(t_1)$ and $T_2 = T_{core}(t_2)$, and $m_{body}(T_{core})$ is the body mass corresponding to body core temperature T_{core}.

Heat lost due to the cap is simply $H_{Loss\_core} - H_{Loss\_saline}$ since these are the only two sources of heat loss in the model. Relative contributions of heat loss, in percentages, were calculated for the following intervals: 0–20, 20–60 min, 1–2, 2–3, 3–4, 4–5, and 5–6 h. The trapezoidal rule was used to calculate integrals in Eqs. (22) and (23).

3. Results

3.1. Failure of cooling cap to induce brain hypothermia

Fig. 3A examines the effect of cooling cap application on the transient temperature profile of the human brain model. One hour after cooling cap application the mean brain temperature was reduced to 36.0 °C. The cooling penetration was very limited. The scalp temperature was reduced to 15.7 °C and only the superficial 5 mm of the gray matter had temperatures within the therapeutic range of hypothermia (Fig. 3B, C). The simulation was discontinued because the brain voxel target temperature (32.0 °C) was not reached after 1 h. During the same period, body temperature was slightly reduced to 36.5 °C.

3.2. Selective brain cooling: ICSI alone or in combination with a cooling cap

Hypothermia induction in the ipsilateral anterior territory (IAT), i.e. the perfusion region of the ipsilateral middle and anterior cerebral arteries, was similar in the model of ICSI alone and the model simulating ICSI and cooling cap application (combination SBC). In both models, the average IAT temperature quickly cooled to therapeutic levels (<33 °C) within approximately 5 min (Fig. 4A). Hypothermia was maintained in both models for the complete 6-h simulation (Fig. 4B).

Fig. 4A shows that body core temperatures gradually decreased during hypothermia maintenance in both models. The reduction in body temperatures is attributed to the cooled jugular venous return to the body core. Moreover, the mild additional cooling effect of the cooling cap to the superficial gray matter in brain tissues other than the IAT resulted in lower jugular venous return temperatures in the combination SBC model compared to the ICSI model (results not shown). This in turn accounts for the lower body core temperatures in the combination SBC model. The body temperature in the combination SBC model reached the

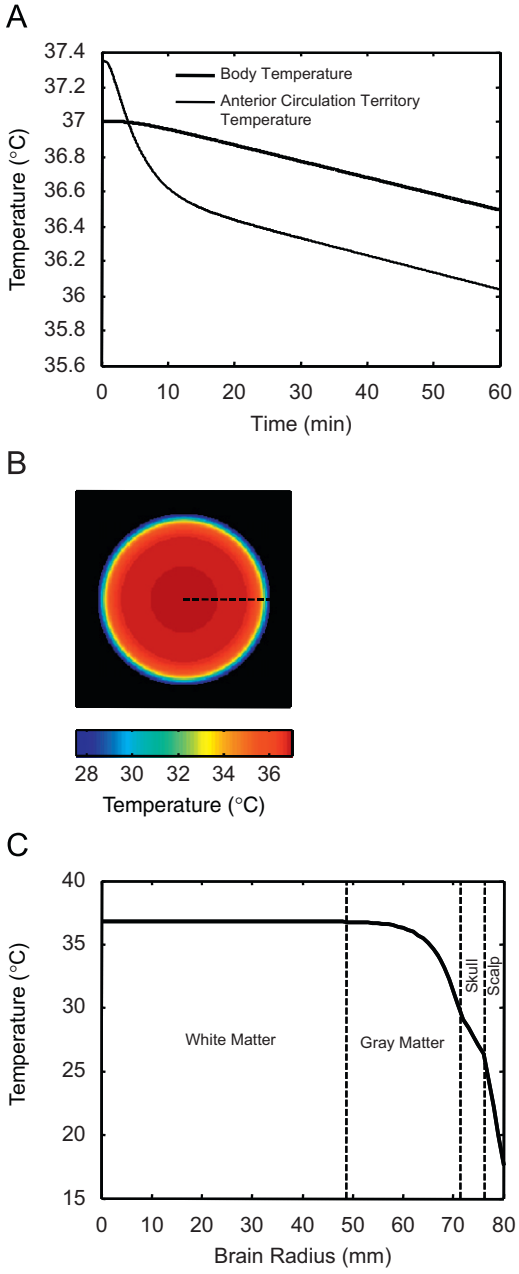

Fig. 3. Failure of cooling cap to induce brain hypothermia. (A) Transient temperature profile. (B) Axial sections of the brain 4.5 cm from the base with the spatial temperature distribution 60 min after cooling cap application. (C) Temperature distribution along the radius drawn in (B).

temperature of cold perfusate in just over 4 h of hypothermia maintenance and both temperatures were equal and decreasing for the remaining time of the simulation.

Fig. 5A shows the transient temperature profile of the cold perfusate flowing in the ICA (i.e., blood and cold saline). The cold perfusate in the combination SBC had a somewhat higher temperature than the perfusate in the ICSI model (32.8 vs. 31.8 °C). Moreover, blood flow rate (including saline flow) in the ipsilateral ICA decreased by 19% and 22% in the ICSI and the combination SBC models, respectively, after 1 h of ICSI (Fig. 5B). The 1 °C difference in perfusate temperatures and the greater reduction in ipsilateral ICA flow reflect the enhancement of brain cooling with the cooling cap; higher perfusate temperatures and lower blood flow rates were adequate for induction and

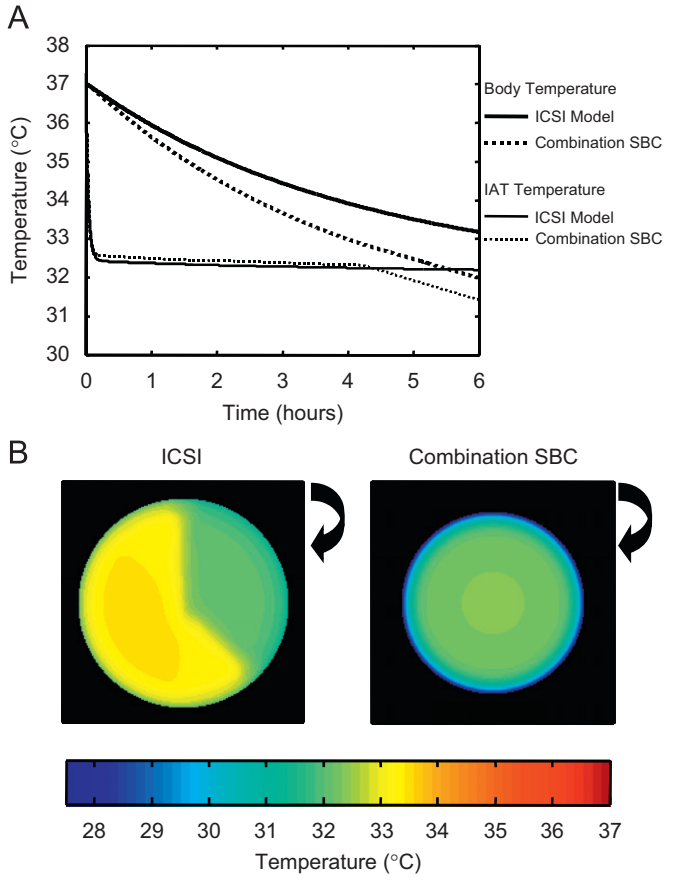

Fig. 4. Temperature in ICSI and combination cooling models. (A) Transient temperature profile of ipsilateral anterior circulation territory (IAT) and body core temperature. (B) Axial sections of the brain 4.5 cm from the base with the spatial temperature distribution 6 h after hypothermia induction.

maintenance of the same level of hypothermia in the combination SBC model.

Fig. 6 shows the relative proportion of cooling contributed by ICSI and the cooling cap for the combination SBC model. ICSI accounted for over 80% of the cooling during hypothermia induction and remained the dominant mode of cooling for the first 3 h. The cooling cap was gradually increasing its cooling contribution and by the fifth hour accounted for 100% of the cooling.

3.3. *Volume loading and hemodilution*

There was a two-phase decrease in ICSI rate. The initial fast phase lasted approximately 5 min as hypothermia was being induced in the IAT (Fig. 7A). Early-phase ICSI rates were high in both models ($>40\,\mathrm{ml\,min^{-1}}$) in order to rapidly cool the perfusate and brain. The subsequent sustained phase resulted in a slower infusion rate reduction. The fast phase mirrors the IAT temperature reduction in the initial 5 min of the simulation; during that period the fast-dropping voxel temperature rapidly decreased the requirements of cold saline infusion. The slow phase decreased in parallel with the reduction of body core temperature. The combination SBC model had lower infusion requirements during hypothermia induction and maintenance (Fig. 7A). It took just over 4 h for the ICSI to stop completely in the combination SBC simulation. This was exactly the same time point where the body core temperature decreased to the level of the perfusate temperature (Figs. 4 and 5) and hypothermia maintenance did not require any saline infusion past that point; cooling was

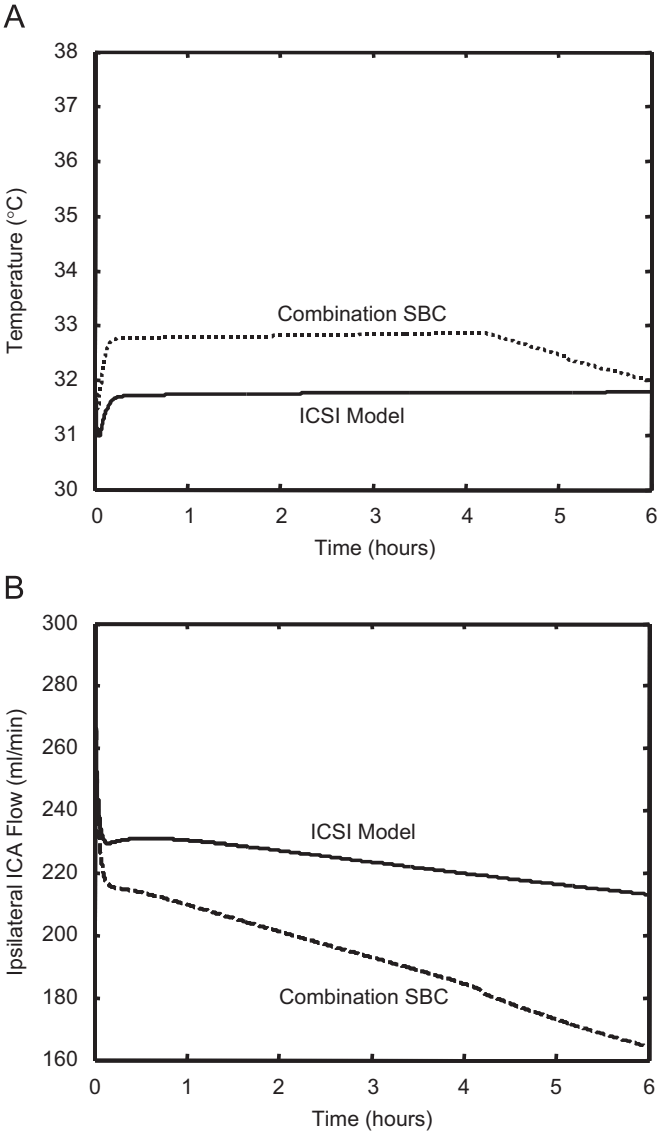

Fig. 5. (A) Perfusate temperature (i.e. ICA and cold saline mixed temperature). (B) Ipsilateral ICA flow (blood and saline) rates for the ICSI model and the combination cooling model.

continued solely with the cooling cap. Continuous saline infusion with flow rates well over $10\,\mathrm{ml\,min^{-1}}$ were required for the ICSI model without cooling cap throughout the entire 6 h simulation.

The higher flow rates for the ICSI model resulted in more than double total volume of infused saline during the 6-h simulation in the ICSI model compared to the combination SBC model (Fig. 7B). A total of 3.3 L were infused in the combination SBC model and 7.5 L in the ICSI model. The large infusion volumes expanded the intravascular volume in the ICSI model, whereas the intravascular volume in the combination SBC was relatively stable during the simulation (Fig. 7B). Fig. 8 shows the evolution of urinary output in the two models. The higher infusion rates accounted for the higher urinary output in the ICSI model.

The effect of hypervolemic hemodilution on hematocrit, with the assumption of an initial hematocrit of 42%, is examined in Fig. 9. The lower infusion rates in the combination SBC model resulted only in a small reduction of systemic hematocrit, which was always maintained above 37%. During the second half of the simulation, where ICSI rates were very low or zero, systemic hematocrit started to increase, approaching 39% after 6 h. In contrast, there was a faster and continuous reduction of systemic

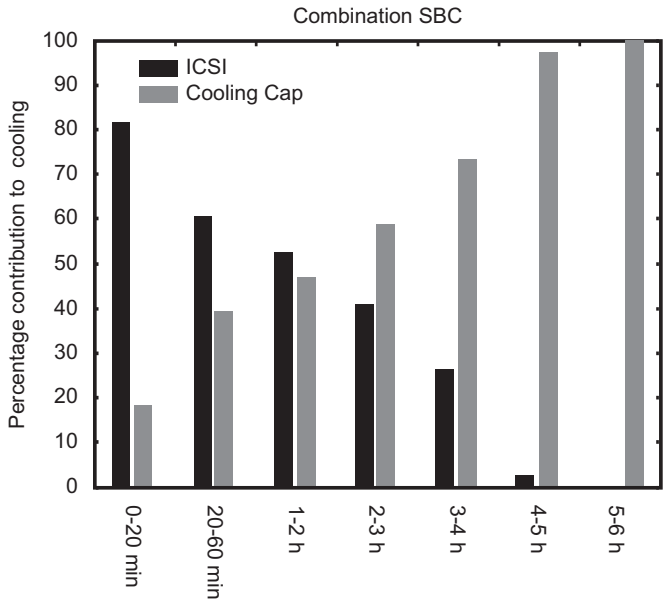

Fig. 6. Percentage contribution to cooling from either ICSI or cooling cap in combination cooling model. The simulation is divided into the induction period (first 20 min), the following 40 min and then into hourly intervals and the relative contribution of ICSI and the cooling cap is shown.

hematocrit in the ICSI model reaching 34% after 6 h. Because of the saline infusion, the hematocrit of the perfusate reaching the brain (local hematocrit) is lower than the systemic hematocrit at any given time since saline is mixing directly with blood in the ICA. Blood supplying ipsilateral ICA regions has a hematocrit represented by local hematocrit values. In the combination SBC model, local hematocrit was always maintained above 35% and after ICSI stopped completely, local and systemic hematocrits were identical. The continuous saline infusion in the ICSI model reduced the local hematocrit to just over 32% after 6 h, this is almost 7% lower than local hematocrit than the combination SBC model.

4. Discussion

4.1. Implications of the results

This study demonstrated similar results to previous studies (Konstas et al., 2007; Neimark et al., 2007) which demonstrated that ICSI has the potential of cooling much more quickly than either closed-circuit venous systems or whole body systemic cooling methods. The control system adds an additional benefit of specifying the rate of cooling, introducing the possibility of more rapid attainment of hypothermia. It is important to note, however, that without warming the body core, it is impossible for any so-called "selective brain cooling" method to completely avoid body core cooling due to VR. However, directly cooling the brain with ISCI is still selective in that a period of 2–3 h of therapy can pass while brain temperatures are at target hypothermia levels, and body core temperatures remain above 35 °C (Fig. 4A).

This study also demonstrates a method of controlling brain temperature in a theoretical model of brain cooling by varying the ICSI rate through a feedback mechanism. With ICSI alone, this method was able to both control the cooling rate and maintain brain temperature at the target level. Maintenance of the target brain temperature was not achieved in the combination SBC model as the feedback mechanism had no way of controlling transcranial cooling through the cooling cap after body temperature reached perfusate temperature (Figs. 4A, 5A) and ICSI flow

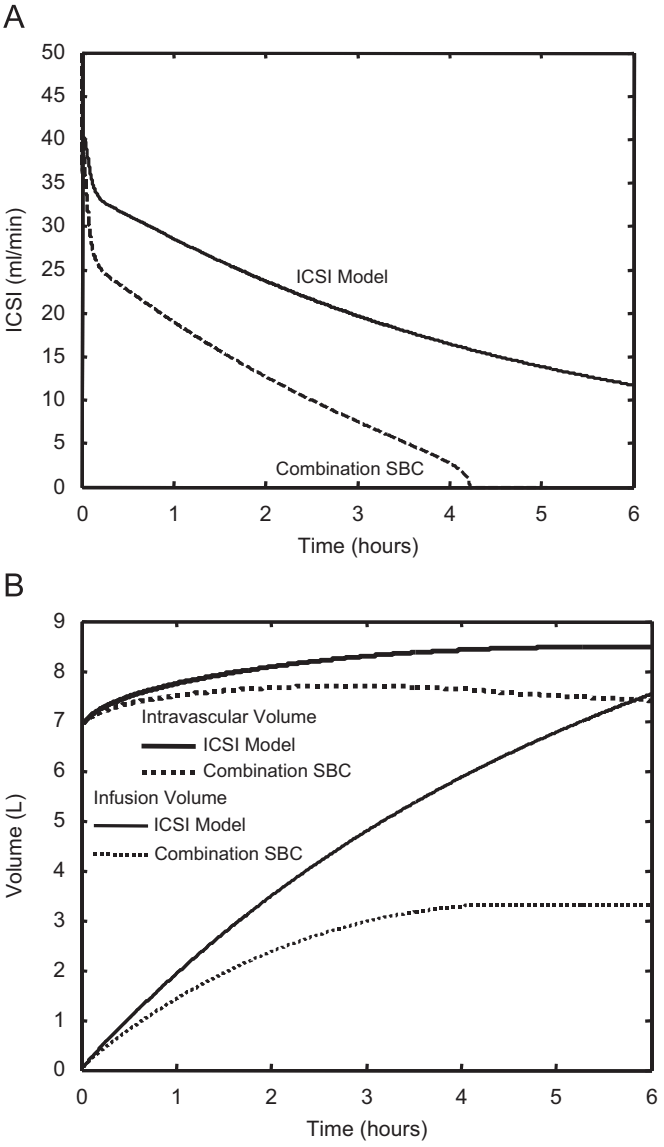

Fig. 7. Volume loading in each model. (A) ICSI flow rates. (B) Cumulative saline infusion volumes and resulting intravascular volumes.

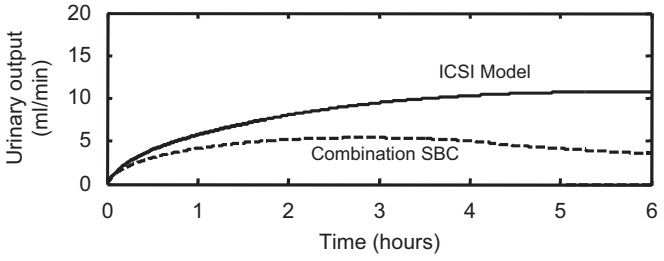

Fig. 8. Urinary output profiles.

rate decreased to zero (Fig. 7A); therefore, IAT and body core temperatures fell below the target level. In clinical practice, the control algorithm could be used with MR thermometry. Studies have shown the feasibility and safety of MR thermometry in monitoring the temperature distributions in patients undergoing microwave ablation of prostate cancer (Chen et al., 2000), and laser-induced interstitial thermotherapy for astrocytomas (Kahn et al., 1998). Another possible option is to directly control

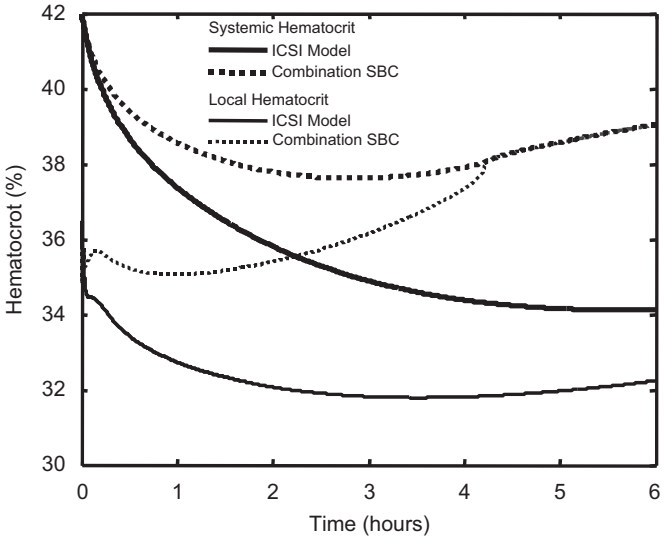

Fig. 9. Effect of saline infusion on hematocrit. Both the systemic and the local (i.e. perfusate) hematocrit are shown for each model.

the temperature of the perfusate (i.e. blood and cold saline mixture) with a thermistor extending from the catheter. Another possibility would be to control saline flow using jugular venous temperature, which could be used to estimate brain temperature in the ICA perfusion regions.

This study confirmed previous theoretical analyses (Diao et al., 2003; Nelson and Nunneley, 1998; Sukstanskii and Yablonskiy, 2007) and empirical measurements (Corbett and Laptook, 1998; Mellergard, 1992; Wang et al., 2004; Zhu et al., 2006) suggesting that transcranial cooling is only effective in reducing the temperature in the superficial regions of the gray matter and not deep brain structures in a timely fashion. Despite the inability of cooling cap to induce hypothermia, the simulations suggested that the cooling cap can enhance brain cooling with ICSI. While the IAT temperature was very close to the target temperature in the ICSI and the combination SBC models, several differences emerged. First, the body core temperature decreased faster in the combination SBC model. Second, the rest of the brain reached lower temperatures in the combination SBC model. Third, lower infusion rates were required for hypothermia induction and maintenance in the combination SBC; cessation of infusion after 4 h maintained brain and body cooling, suggesting that the cooling cap alone can maintain both SBC and systemic hypothermia past this point. All these differences are summarized by the different profile of cooling contribution in the combination SBC model. ICSI contributed over 80% for hypothermia induction, whereas the cooling cap contributed 100% to hypothermia maintenance during the last hour of the simulation.

Although the cooling cap was unable to achieve therapeutic hypothermia on its own, there was a remarkable enhancement of cooling in conjunction with ICSI, which surpassed the cooling ability of ICSI alone, as demonstrated by the 55% reduction of volume necessary to maintain brain temperature at the same temperature. These contrasting results can be explained by several factors. First of all, the cooling cap contributed significantly to cold venous return which reduced core body temperature. Although at first its contribution was only about 20% of cooling, its effect remained steady while cold saline flow dropped over the course of the simulation. For this reason, body core temperatures decreased more rapidly in the combined ICSI cooling cap model than in the model employing ICSI alone (Fig. 4A). Second, by reducing brain CBF, the cooling cap limited the amount of cold saline necessary to maintain perfusate temperature at its necessary temperature. The temperature of the incoming arterial blood is the main determinant of brain temperature under steady-state conditions (Hayward and Baker, 1968; Zhu et al., 2006). Although, ICSI decreased intracerebral temperatures resulting in overall reduction of CBF (and hence ICA flow), the addition of the cooling cap cooled brain temperatures even further, reducing ICA flow beyond ICSI alone (Fig. 5B). This limited the necessary amount of cold saline to maintain brain temperature at the controlled level. A third reason for the ability of the cooling cap to enhance controlled hypothermia was its ability to cool the brain directly, thereby not requiring as cool perfusate temperatures (Fig. 5A).

The reduction of the total infused volume by over 55% and the minimization of intravascular volume expansion and hemodilution during the 6-h simulation period with the combination SBC have important clinical implications. A large proportion of patients with acute ischemic stroke have other co-morbidities, such as ischemic heart disease, congestive heart failure and renal dysfunction (Johansen et al., 2006; Koren-Morag et al., 2006). Intravascular volume expansion and hemodilution may be detrimental for these patients and counteract the beneficial effect of therapeutic hypothermia. Thus, combination SBC may be a safer method of hypothermia induction and maintenance in these patients.

4.2. Limitations of the models

The present model has several limitations. (1) The present model assumes constant and equal rates of heat transfer loss and heat generation inside the body. In reality, hypothermia-induced shivering will disturb this equilibrium and heat generation will exceed loss, resulting in a possible overestimation of body core cooling from the cooled jugular venous return. As a result, higher rates of ICSI may be needed for hypothermia maintenance in the ICSI model and it is possible that the cooling cap alone may not be able to maintain hypothermia in the combination SBC; instead low infusion rates may always be required. However, two lines of evidence support the predictions made by our models. First, induction of thermoregulatory tolerance with antishivering medications will minimize hypothermia-induced shivering. Several studies have demonstrated that anesthetics, muscle relaxants and opioids produce substantial decreases in the shivering thresholds. Propofol, desflurane and meperidine each decrease the shivering threshold from 36.5 °C to even less than 32 °C (Kurz et al., 1997; Sessler, 1997). Hence, antishivering medications will deactivate the thermoregulatory responses of patients undergoing SBC and will make the patients poikilothermic throughout the range of body temperatures achieved in our simulations. Second, data from intravenous cold infusion studies suggest that for modest systemic temperature drops use of antishivering drugs is associated with temperature decreases greater than what would be theoretically predicted with our model; in groups of patients not treated with antishivering medications the average difference between the actual and predicted systemic temperature drop was 0.0 °C (Neimark et al., 2007). The comparison of human data with our simulations supports the predictions of our models. (2) The incracranial anatomy was simplified as the geometry of the head was modeled as a hemisphere. However, a careful selection of appropriate dimension yielded a brain volume of 1285 ml, a value half way between the average male and female brain (Koh et al., 2005) (3) The Pennes' equation describes a continuum model where heat and mass transport are averaged over a representative unit volume. Continuum models are not able to predict the variation in temperature in the immediate vicinity of large, discrete blood vessels. However, the results obtained from a discrete vessel thermal model agreed well with Pennes'

continuum model (Van Leeuwen et al., 2000). (4) In the model it is assumed that the dependence of CBF on local temperature and hematocrit is the same as that for global temperature and hematocrit. Several animal experiments (Ibayashi et al., 2000; Laptook et al., 2001; Walter et al., 2000) have confirmed that there are not significant differences in the reduction of CBF between systemic cooling and selective brain cooling. Although, to the best of our knowledge, there are no similar studies investigating potential differences between local and systemic hemodilution, it is reasonable to assume that perfusion increases due to hemodilution are also locally mediated. Further, a feline study has reported that vascular responses to oxygenation changes in the brain are locally mediated and occur within 3 s (Malonek and Grinvald, 1996).

In conclusion, this study presents a method of controlling brain temperature in SBC. The results suggest that ICSI can maintain stable levels of therapeutic hypothermia for 6 h. Moreover, while confirming the inability of cooling caps to induce significant SBC, this is the first study supporting a role in maintaining SBC with cooling caps.

Acknowledgements

This study has been supported by a generous grant from the Dana Foundation.

Appendix A. Derivation of Eq. (19)

For a cylindrical catheter, the heat transfer rate across the catheter wall is (Slotboom et al., 2004)

$$\dot{Q} = hA_{cath}\frac{\Delta T_{in} - \Delta T_{out}}{\ln(\Delta T_{in}/\Delta T_{out})} \quad (A.1)$$

where ΔT_{in} is $T_{core}-T_{saline\_in}$ (where T_{saline_in} is the saline temperature infused at the entrance of the catheter) and ΔT_{out} is $T_{core}-T_{saline}$. A_{cath} is the area of the cylindrical catheteral wall. The decrease in temperature of saline along the catheter is also related to heat transfer according to

$$\dot{Q} = F_{saline}\rho_{saline}c_{saline}(T_{saline} - T_{saline\_in}) \quad (A.2)$$

Equating Eqs. (A.1) and (A.2) one obtains the following expression:

$$\frac{hA_{cath}}{F_{saline}\rho_{saline}c_{saline}} = \ln\left(\frac{T_{core} - T_{saline\_in}}{T_{core} - T_{saline}}\right) \quad (A.3)$$

Taking the exponential of both sides of Eq. (A.3) and then rearranging, one obtains

$$T_{saline} = (T_{saline\_in} - T_{core})e^{-hA_{cath}/F_{saline}\rho_{saline}c_{saline}} + T_{core} \quad (A.4)$$

Since h_{cath}, ρ_{saline}, A_{cath}, and c_{saline} are assumed to be constant throughout the infusion, they are combined to a single normalized heat transfer constant, H_{cath}. Outflow saline temperature is then determined as

$$T_{saline} = (T_{saline\_in} - T_{core})e^{-H_{cath}/F_{saline}} + T_{core} \quad (A.5)$$

which is Eq. (19).

References

Baish, J.W., 2000. Microvascular heat transfer. In: Bronzio, J.D., Joseph, D. (Eds.), The Biomedical Engineering Handbook, second ed. vol. 2, CRC, Boca Raton, FL, pp. 98-1–98-14.

Bernard, S.A., Gray, T.W., Buist, M.D., Jones, B.M., Silvester, W., Gutteridge, G., Smith, K., 2002. Treatment of comatose survivors of out-of-hospital cardiac arrest with induced hypothermia. New Engl. J. Med. 346, 557–563 (see comment).

Chen, H., Chopp, M., Zhang, Z.G., Garcia, J.H., 1992. The effect of hypothermia on transient middle cerebral artery occlusion in the rat. J. Cereb. Blood Flow Metab. 12, 621–628.

Chen, J.C., Moriarty, J.A., Derbyshire, J.A., Peters, R.D., Trachtenberg, J., Bell, S.D., Doyle, J., Arrelano, R., Wright, G.A., Henkelman, R.M., Hinks, R.S., Lok, S.Y., Toi, A., Kucharczyk, W., 2000. Prostate cancer: MR imaging and thermometry during microwave thermal ablation-initial experience. Radiology 214, 290–297.

Childs, C., Hiltunen, H., Vidyasagar, R., Kauppinen, R.A., 2007. Determination of regional brain temperature using proton magnetic resonance spectroscopy to assess brain-body temperature differences in healthy human subjects. Magn. Reson. Med. 57, 59–66.

Corbett, R.J., Laptook, A.R., 1998. Failure of localized head cooling to reduce brain temperature in adult humans. Neuroreport 9, 2721–2725.

De Georgia, M.A., Krieger, D.W., Abou-Chebl, A., Devlin, T.G., Jauss, M., Davis, S.M., Koroshetz, W.J., Rordorf, G., Warach, S., 2004. Cooling for Acute Ischemic Brain Damage (COOL AID): a feasibility trial of endovascular cooling. Neurology 63, 312–317.

Diao, C., Zhu, L., Wang, H., 2003. Cooling and rewarming for brain ischemia or injury: theoretical analysis. Ann. Biomed. Eng. 31, 346–353.

Drobin, D., Hahn, R.G., 2002. Kinetics of isotonic and hypertonic plasma volume expanders. Anesthesiology 96, 1371–1380.

Ehrlich, M.P., McCullough, J.N., Zhang, N., Weisz, D.J., Juvonen, T., Bodian, C.A., Griepp, R.B., 2002. Effect of hypothermia on cerebral blood flow and metabolism in the pig. Ann. Thorac. Surg. 73, 191–197.

Feigin, V., Anderson, N., Gunn, A., Rodgers, A., Anderson, C., 2003. The emerging role of therapeutic hypothermia in acute stroke. Lancet Neurol. 2, 529 (comment).

Fiala, D., Lomas, K.J., Stohrer, M., 1999. A computer model of human thermoregulation for a wide range of environmental conditions: the passive system. J. Appl. Physiol. 87, 1957–1972.

Georgiadis, D., Schwarz, S., Kollmar, R., Schwab, S., 2001. Endovascular cooling for moderate hypothermia in patients with acute stroke: first results of a novel approach. Stroke 32, 2550–2553.

Harris, B.A., Andrews, P.J.D., 2005. Direct brain cooling. In: Mayer, S.A., Sessler, D.I. (Eds.), Therapeutic Hypothermia. Marcel Dekker, New York, pp. 323–386.

Hayward, J.N., Baker, M.A., 1968. Role of cerebral arterial blood in the regulation of brain temperature in the monkey. Am. J. Physiol. 215, 389–403.

Ibayashi, S., Takano, K., Ooboshi, H., Kitazono, T., Sadoshima, S., Fujishima, M., 2000. Effect of selective brain hypothermia on regional cerebral blood flow and tissue metabolism using brain thermo-regulator in spontaneously hypertensive rats. Neurochem. Res. 25, 369–375.

Johansen, H.L., Wielgosz, A.T., Nguyen, K., Fry, R.N., 2006. Incidence, comorbidity, case fatality and readmission of hospitalized stroke patients in Canada. Can. J. Cardiol. 22, 65–71.

Kahn, T., Harth, T., Kiwit, J.C., Schwarzmaier, H.J., Wald, C., Modder, U., 1998. In vivo MRI thermometry using a phase-sensitive sequence: preliminary experience during MRI-guided laser-induced interstitial thermotherapy of brain tumors. J. Magn. Reson. Imag. 8, 160–164.

Kammersgaard, L.P., Rasmussen, B.H., Jorgensen, H.S., Reith, J., Weber, U., Olsen, T.S., 2000. Feasibility and safety of inducing modest hypothermia in awake patients with acute stroke through surface cooling: a case-control study: the Copenhagen Stroke Study. Stroke 31, 2251–2256.

Koh, I., Lee, M.S., Lee, N.J., Park, K.W., Kim, K.H., Kim, H., Rhyu, I.J., 2005. Body size effect on brain volume in Korean youth. Neuroreport 16, 2029–2032.

Konstas, A.A., Choi, J.H., Pile-Spellman, J., 2006. Neuroprotection for ischemic stroke using hypothermia. Neurocrit. Care 4, 168–178.

Konstas, A.A., Neimark, M.A., Laine, A.F., Pile-Spellman, J., 2007. A theoretical model of selective cooling using intracarotid cold saline infusion in the human brain. J. Appl. Physiol. 102, 1329–1340.

Koren-Morag, N., Goldbourt, U., Tanne, D., 2006. Renal dysfunction and risk of ischemic stroke or TIA in patients with cardiovascular disease. Neurology 67, 224–228.

Krieger, D.W., De Georgia, M.A., Abou-Chebl, A., Andrefsky, J.C., Sila, C.A., Katzan, I.L., Mayberg, M.R., Furlan, A.J., 2001. Cooling for acute ischemic brain damage (cool aid): an open pilot study of induced hypothermia in acute ischemic stroke. Stroke 32, 1847–1854.

Kurz, A., Ikeda, T., Sessler, D.I., Larson, M.D., Bjorksten, A.R., Dechert, M., Christensen, R., 1997. Meperidine decreases the shivering threshold twice as much as the vasoconstriction threshold. Anesthesiology 86, 1046–1054.

Laptook, A.R., Shalak, L., Corbett, R.J., 2001. Differences in brain temperature and cerebral blood flow during selective head versus whole-body cooling. Pediatrics 108, 1103–1110.

Lyden, P.D., Allgren, R.L., Ng, K., Akins, P., Meyer, B., Al-Sanani, F., Lutsep, H., Dobak, J., Matsubara, B.S., Zivin, J., 2005. Intravascular cooling in the treatment of stroke (ICTuS): early clinical experience. J. Stroke Cerebrovasc. Dis. 14, 107–114.

Malonek, D., Grinvald, A., 1996. Interactions between electrical activity and cortical microcirculation revealed by imaging spectroscopy: implications for functional brain mapping. Science 272, 551–554.

Mellergard, P., 1992. Changes in human intracerebral temperature in response to different methods of brain cooling. Neurosurgery 31, 671–677.

Michenfelder, J.D., Milde, J.H., 1991. The relationship among canine brain temperature, metabolism, and function during hypothermia. Anesthesiology 75, 130–136.

Neimark, M.A., Konstas, A.A., Laine, A.F., Pile-Spellman, J., 2007. Integration of jugular venous return and circle of Willis in a theoretical human model of selective brain cooling. J. Appl. Physiol. 103, 1837–1847.

Nelson, D.A., Nunneley, S.A., 1998. Brain temperature and limits on transcranial cooling in humans: quantitative modeling results. Eur. J. Appl. Physiol. 78, 353–359.

Pennes, H.H., 1948. Analysis of tissue and arterial blood temperature in the resting human forearm. J. Appl. Physiol. 1, 93–122.

Schwab, S., Georgiadis, D., Berrouschot, J., Schellinger, P.D., Graffagnino, C., Mayer, S.A., 2001. Feasibility and safety of moderate hypothermia after massive hemispheric infarction. Stroke 32, 2033–2035 (see comment).

Sessler, D.I., 1997. Mild perioperative hypothermia. New Engl. J. Med. 336, 1730–1737.

Slotboom, J., Kiefer, C., Brekenfeld, C., Ozdoba, C., Remonda, L., Nedeltchev, K., Arnold, M., Mattle, H., Schroth, G., 2004. Locally induced hypothermia for treatment of acute ischaemic stroke: a physical feasibility study. Neuroradiology 46, 923–934.

Sukstanskii, A.L., Yablonskiy, D.A., 2007. Theoretical limits on brain cooling by external head cooling devices. Eur. J. Appl. Physiol.

The Hypothermia After Cardiac Arrest (HACA) Study Group, 2002. Mild therapeutic hypothermia to improve the neurologic outcome after cardiac arrest. New Engl. J. Med. 346, 549–556.

The National Institute of Neurological Disorders and Stroke rt-PA Stroke Study Group, 1995. Tissue plasminogen activator for acute ischemic stroke. New Engl. J. Med. 333, 1581–1587.

Van Leeuwen, G.M., Hand, J.W., Lagendijk, J.J., Azzopardi, D.V., Edwards, A.D., 2000. Numerical modeling of temperature distributions within the neonatal head. Pediatr. Res. 48, 351–356.

Walter, B., Bauer, R., Kuhnen, G., Fritz, H., Zwiener, U., 2000. Coupling of cerebral blood flow and oxygen metabolism in infant pigs during selective brain hypothermia. J. Cereb. Blood Flow Metab. 20, 1215–1224.

Wang, H., Olivero, W., Lanzino, G., Elkins, W., Rose, J., Honings, D., Rodde, M., Burnham, J., Wang, D., 2004. Rapid and selective cerebral hypothermia achieved using a cooling helmet. J. Neurosurg. 100, 272–277.

Zhu, M., Ackerman, J.J., Sukstanskii, A.L., Yablonskiy, D.A., 2006. How the body controls brain temperature: the temperature shielding effect of cerebral blood flow. J. Appl. Physiol. 101, 1481–1488.